2021

Drastic enhancement of CO2 adsorption capacity by negatively charged sub-bituminous coal

Hussein R. Abid
Edith Cowan University

Stefan Iglauer
Edith Cowan University

Ahmed Al-Yaseri
Edith Cowan University

Alireza Keshavarz
Edith Cowan University

10.1016/j.energy.2021.120924
Abid, H. R., Iglauer, S., Al-Yaseri, A., & Keshavarz, A. (2021). Drastic enhancement of CO2 adsorption capacity by negatively charged sub-bituminous coal. *Energy, 233,* article 120924. https://doi.org/10.1016/j.energy.2021.120924

Energy 233 (2021) 120924

Contents lists available at ScienceDirect

Energy

journal homepage: www.elsevier.com/locate/energy

Drastic enhancement of CO_2 adsorption capacity by negatively charged sub-bituminous coal

Hussein Rasool Abid [a, b, **], Stefan Iglauer [a], Ahmed Al-Yaseri [a], Alireza Keshavarz [a, *]

[a] School of Engineering, Edith Cowan University, 270 Joondalup Drive, Joondalup, WA, 6027, Australia
[b] Environmental Department, Applied Medical Science, University of Karbala, Karbala, 56001, Iraq

ARTICLE INFO

Article history:
Received 25 February 2021
Received in revised form
7 May 2021
Accepted 10 May 2021
Available online 31 May 2021

Keywords:
CO_2 storage
Coal
Adsorption
Chemical modification
Methyl orange

ABSTRACT

Climate change is a key problem of the 21st century. Climate change is mainly caused by anthropogenic CO_2 emissions, and one solution to this problem is to capture and store CO_2 in deep coal seams, where it is immobilized by adsorption to the coal surface. Here we propose to modify the coal with methyl orange (MO), a typical dye that is also a major pollutant of the hydrosphere and removed thereby. Thus, raw and MO-modified coals were characterized to investigate their thermal stabilities, textural properties, carbon contents, surface characteristics, and CO_2 adsorption on the coal samples was measured at typical storage conditions (323 K and pressures up to 37.5 bar). CO_2 adsorption dramatically increased in the MO-coal, from 1.95 mol. kg^{-1} (raw coal) to 18.7 mol. kg^{-1}.

This work thus aids in the development of improved methods for CO_2 storage, to significantly mitigate climate change.

1. Introduction

Anthropogenic CO_2 emissions to the atmosphere are a key problem of the 21st century as they cause global warming and consequently climate change [1]. Fossil fuel, such as oil and coal is a main source of energy throughout the world therefore the greenhouse gases such as CO_2 and CH_4 have been emitted as this fuel consumed for human activities [2–4]. To reduce CO_2 emissions to the atmosphere, different techniques have been used; sorption processes have been applied via physical and chemical methods [5,6]. Also, fuel modifications, using CO_2 produced in industry, and using clean energy resources are still targeted for that purpose [7]. However, these methods are not sufficient to reduce the accumulated concentration of CO_2 from the atmosphere to standard levels. Therefore, modern countries have focused on deep ocean and geological sequestrations [8]. Recently, depleted oil and gas reservoirs have been widely used as bulky tanks for storing CO_2 gas [9–11,68,69]. Besides, deep underground coal seams have been used to drastically reduce these CO_2 emissions, and to capture and store CO_2 [12–17]. The storage capacity of a deep coal seam is thus directly linked to its CO_2-adsorption capacity at high pressures (note that pressure in the subsurface increases with depth due to hydrostatic and overburden pressures) [18]. The adsorption capacity depends on the applied pressure; note that typical pressures prevailing in deep coal seams range from 35 to 60 bar [19] as coal seam depths are normally shallow when compared to oil reservoirs [20]. Typical CO_2-adsorption capacities range between 0.6 and 1.9 mol. kg^{-1} depending on the temperature, pressure, and coal rank [21]. Numerous chemical modifications have been used to improve physiochemical properties of porous materials and consequently enhancing their affinity toward adsorption of CO_2 [22,23]. The chemical and physical characteristics of coal are a prime factor that might affect the CO_2 adsorption on coal [10,24]. Accordingly, to enhance the CO_2 adsorption capacity on the coal, the modification of the surface and pore structure of the coal by inserting other materials is required. However, a scientific inquire about the ability of researchers to insert other chemicals into the pore structure of the coal to increase its affinity to adsorb CO_2 has been currently emerged [25,26]. That means the study of enhancing CO_2 adsorption on the coal by inserting another chemical is still not gotten birth yet. Because the coal is classified as a porous material enriched with abundant oxygen functional groups, it has been used as an outstanding adsorbent to remove dyes from wastewater [27]. Dual treatment is now important to seizure dyes in the coal

* Corresponding author.
** Corresponding author. School of Engineering, Edith Cowan University, 270 Joondalup Drive, Joondalup, WA, 6027, Australia.
E-mail addresses: h.alfatlawi@ecu.edu.au (H.R. Abid), a.keshavarz@ecu.edu.au (A. Keshavarz).

https://doi.org/10.1016/j.energy.2021.120924

reservoir and consequently to increase the total amount of CO_2 which can be stored there. Methyl orange (MO), a classic dye used in various industries such as textile, paper, rubber, cosmetic, wool, and nylon industry [28–32]. MO is therefore a major pollutant that is discharged into the hydrosphere in large quantities [33,34] – however, it can be efficiently adsorbed on the coal [35]. Here we propose to prime coal with methyl orange (MO). The target of this study is to enhance the density of ionic charge on the surface of the pores in the coal structure which can significantly improve the adsorptive characteristics of the coal toward increasing the adsorption capacity of CO_2. Crucial characterization of the coal samples is reported. CO_2 adsorption at conditions near to the reservoir conditions is carried out for the coal sample before and after the modification. As described in detail below, this MO-priming dramatically increases CO_2 adsorption capacities of coal – this work thus aids in the development of improved methods for CO_2 storage, to significantly mitigate climate change.

2. Materials and methods

2.1. Materials and sample preparation

Sub-bituminous coal (Pan Upper; maximum vitrinite reflectance: 0.38%) was supplied by Premier Coal (Collie, Western Australia), the coal properties were measured, and essential analysis; Proximate, Petrographic and Ultimate Analysis of coal samples were performed by Bureau Veritas Mineral Pty Ltd (NSW, Australia) and the results are tabulated in Table 1. Methyl orange (MO; $C_{14}H_{14}N_3NaO_3S$, dye content 85 wt%; Fig. 1) was supplied by Sigma Aldrich, and deionized ultrapure water was produced via a Membrane RO100 instrument (Aquatec-CDP-8800- USA). The coal samples were first crushed with a blade grinder (700G high speed chinses electric medicine crusher) to produce fine powders. The powder was sieved with a sieve shaker (Analyser- Endicotts EFL 300) to a homogenous powder with a suitable particle size (<250 μm). The powder was initially washed by DI water to leach salt (NaCl) out. A 250-ppm methyl orange solution was then prepared in DI water (the average pH value was 8.7 measured with a Portable pH/conductivity meter-WP-90), and 1.5 g of the raw coal was dispersed in 40 mL of the methyl orange solution with ongoing mixing for 3 days. Subsequently, the resulting MO-coal powder was separated from the dispersion via vacuum filtration. The sample was dried in a preheated oven at 60 °C for 3 days. Finally, the MO-coal was degassed under vacuum using a VacPrep 061-Micromeritics system for 2 h at 343 K prior to the adsorption experiments. Zeta potentials of the raw coal and the MO coal powders were measured with a Zetasizer Nano- ZS instrument (Malvern Panalytical Company, Australia) (S1).

Table 1
Essential analysis properties of Pan upper raw coal.

Approximate Analysis			
Moisture Content (wt%)	Ash Content (wt%)	Volatile Content (wt%)	Fixed Carbon (wt%)
21.1	2.5	28.0	47.8
Petrographic Analysis			
Vitrinite (Vol %)	Liptinite (Vol %)	Inertinite (Vol %)	Mineral Matter (Vol %)
33.3	11.3	43.9	11.5
Ultimate Analysis			
Carbon (wt%)	Hydrogen (wt%)	Nitrogen (wt%)	Relative Density
58.1%	2.98%	1.15%	1.39

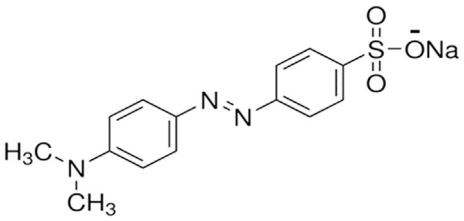

Fig. 1. Chemical structure of Methyl Orange.

2.2. Coal characterization

The decomposition temperature of the raw and MO-coals was measured via thermal gravimetric analysis (TGA) using a PerkinElmer-Thermogravimetric Analyzer-TGA 4000 (S.2). Furthermore, FTIR spectra were measured with a PerkinElmer-FT-IR Spectrometer (Model 100-FT-IR), and N_2 (Coregas, HPG, purity = 99.99 vol%) adsorption-desorption measurements were performed (at 77 K) to determine the BET (Brunauer, Emmett and Teller) surface areas and pore size distributions (using the Tristar II 3020) (S.3). Carbon content was measured with an elemental analyzer (PerkinElmer, Series II-CHNS/O Analyzer), and energy-dispersive X-ray mapping was performed with a Hitachi SU3500 Scanning Electron Microscope.

2.3. High pressure adsorption study

Pure CO_2 (purity = 99.99 vol %), He (HPG, purity = 99.99 vol **%)** and Air (Instrument Grade- Compressed, purity = 99.995 vol %) were supplied by Coregas. CO_2 was the adsorbate gas, while He was used to calibrate the void volume of the sample and to check the gas leakage. Air was used to operate the valves of the adsorption instrument pneumatically. The high-pressure adsorption measurements were performed on a PCTpro adsorption analyzer (Setaram Instrumentation, Figure S2) (S.4). The measurements were repeated three times; the standard error ranged from ±0.047 at 2.7 bar to ±0.102 at around 37 bar for CO_2 adsorption measurements in raw coal and it was ranged from ±0.079 at 5 bar to ±0.24 at around 37 bar in MO-coal.

3. Results and discussion

3.1. Coal modification with methyl orange

80 wt % of MO was incorporated into the raw coal (5.33 mg. g^{-1}, (S5, Figure S3)) by non-covalent π-π interactions between the polycyclic aromatic rings (present in the coal) and the phenyl rings in the MO; in addition, hydrogen bonding between MO nitrogen atoms and hydroxyl groups of coal might have further enhanced adsorption [35–38]. Furthermore, it was established earlier that higher negative charge densities on the coal surface decrease MO adsorption [39,40]. Consequently, in comparison with Methylene Blue (MB) [27], the adsorption rate of MO on the tested raw coal was relatively low because this untreated coal had a very low zeta potential of −70 ± 0.88 mV at pH 8.7. This is consistent with literature data [41–43]. The zeta potential increased to − 60 ± 1.5 mV in the MO-coal due to the incorporation of MO into the coal matrix; therefore, the concentration of ionizable chemical groups on the MO-coal surface was higher than that on the raw coal; consequently, the adsorption capacity of the coal toward Lewis acid adsorbates was enhanced [44,45]. EDX mapping demonstrated that sodium (Na) was an indicator of MO incorporation into the MO-coal, Fig. 2a–c. The main source of Na in the raw coal was the

sodium chloride initially present into the raw coal, which was leached out of the raw coal during MO-coal preparation as shown in Fig. 2a and b, respectively. Furthermore, the carbon content increased after MO modification (from 60 wt % to 65 wt %). MO incorporation into the coal was also confirmed by FTIR, thus the sulfonic groups of the MO were detected in the coal, Fig. 3. Note that the sulfonic group is recognized by two peak clusters, namely the peaks at 685 and 755 cm^{-1} (which are related to the C–S stretching vibrations) and the peaks at 913, 1032 and 1091 cm^{-1} (which are related to the SO_3^- stretching vibrations). In addition, the peaks at 2850 and 2923 cm^{-1} were caused by C–N bond vibrations and asymmetric CH_3 stretching vibrations – mainly caused by the incorporation of MO [46]. Moreover, the peaks at 1373 and 1434 cm^{-1} were caused by the N=N stretching vibration which increased with MO content, again confirming the incorporation of MO into the coal. The peaks at 1229 and 1592 cm^{-1} are linked to CH_3 and C=C stretching vibrations, respectively, which were also enhanced in MO-coal. Finally, the peak at 1698 cm^{-1} was caused by the C=O stretching of aromatic rings in the raw coal [47,48].

Furthermore, during TGA analysis, the raw coal experienced a two-step weight loss, Figure S1. Initially (first step) moisture content was released when the temperature increased to 330 K; subsequently, (second step) the organic matter (macerals) in the coal started to degrade at 580 K; this is consistent with the results reported by Buratti et al. (2015) and Saikia et al. (2008) [49,50]. However, MO-coal experienced three weight loss steps; in addition to moisture loss (330–376 K) and maceral degradation (550–683 K), the MO molecules were pyrolyzed at 720 K. Interestingly, the MO-coal had higher thermal stability (749–834 K) than the raw coal (550–720 K), apparently due to the incorporation of MO into the coal structure.

Moreover, both, raw coal and MO-coal showed hysteresis in their N_2 adsorption/desorption isotherms; Fig. 4a and b. This hysteresis was more significant in raw coal. Hence, ink-bottle pores were dominated in raw coal because the diameter of the mesopore was equal to the critical diameter of hysteresis (4 nm for N_2 at 77 K). N2 isotherm shows that with increasing relative pressure, N_2 condensed first in the pore necks, followed by N_2 condensation in the pore cavities [51,52]. However, when the relative pressure

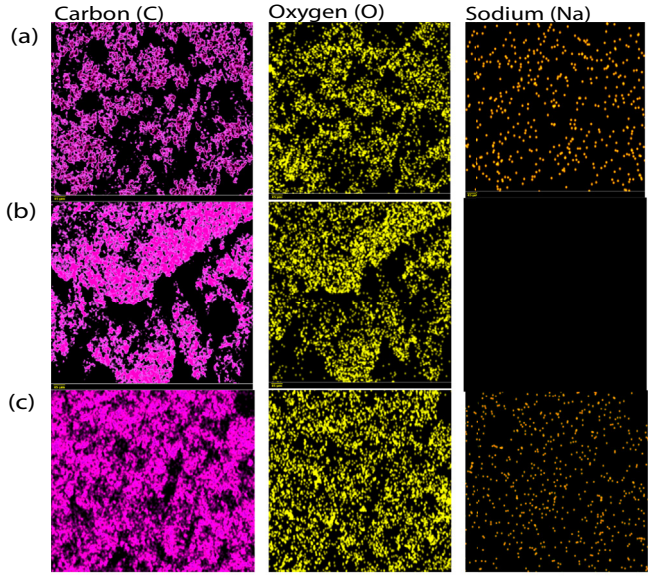

Fig. 2. Energy-dispersive x-ray spectrographic mapping of C, O and Na on a) raw coal, b) raw coal after washing with DI water and c) MO-coal.

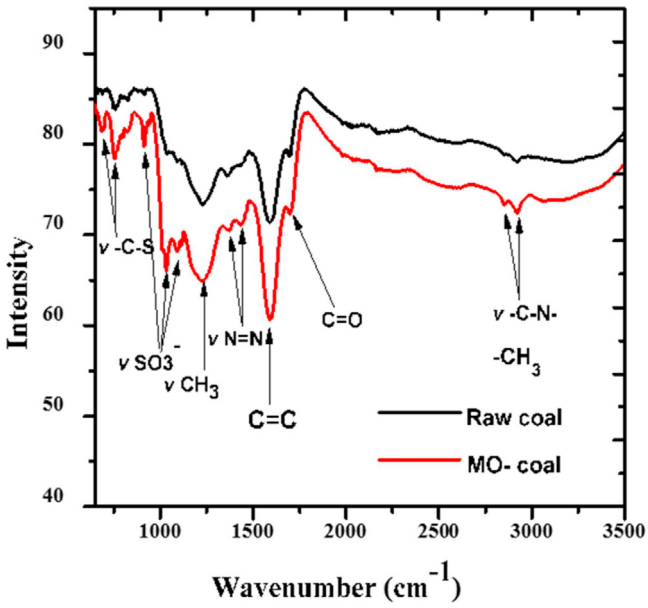

Fig. 3. Fourier-transformed infrared spectra of raw coal and MO-coal.

decreased during desorption, slow evaporation emptied pore bodies and pore throats simultaneously [53,54]. The sharper rise in the MO-coal adsorption isotherms (when the relative pressure approached unity) indicated a higher percentage of macropores [5,55]. Noteworthy, during the pre-treatment of coal by deionized water, chloride salts were dissolved, therefore the coal network was enriched by vacant sites for MO adsorption. Consequently, the diffusion rate of MO via coal was increased and might create new pores. Accordingly, the specific surface area increased from 5.70 $m^2.g^{-1}$ in the raw coal to 7.02 $m^2.g^{-1}$ in the MO-coal, the pore volume did not change (it was 0.02 cc. g^{-1} for both coal types). Furthermore, the average pore size decreased slightly in the MO-coal, from 13.82 nm (in the raw coal) to 12.99 nm, consistent with a decrease in mesopore size (from 4 to 2.75 nm in the raw coal to 3.50 and 2.50 nm in the MO-coal), Fig. 4c.

3.2. CO_2 adsorption

The CO_2 adsorption capacity of the raw coal dramatically increased by MO modification, from 1.95 mol. kg^{-1} to 18.7 mol. kg^{-1} (at 323 K and 37.5 bar), Fig. 5.

We hypothesize that this drastic increase in CO_2 adsorption was due to the negatively charged MO incorporated into the coal pores. This increase in the negative surface charge density strongly attracted the CO_2 molecules [56], due to their high quadrupole moment ($-13{\cdot}4 \pm 0{\cdot}4 \times 10^{-40}$ C m^2); compare Zou and Rodrigues (2001) or Iglauer (2017) [57,58]. Mechanistically, the positive carbon atom in the (stiff and linear) CO_2 molecule interacts with the negative surface charge and orients the CO_2 molecules parallel to the adsorbent's surface [59]. This flat adsorption profile significantly enhances CO_2–CO_2 intermolecular interaction [60]. This effect was further enhanced by the increased surface area and slightly reduced pore size in the MO coal (see above); and recall that CO_2 adsorption increases with higher surface area and smaller pore sizes; [61,62]. In addition, secondary van der waals interaction between the nitrogen atoms of incorporated MO in MO-coal and carbon atoms of CO_2 molecules highly contributed to increase the CO_2 adsorption capacity [63]. Finally, carbon is an imperative constituent of organic matter in coal. It represents the main element of

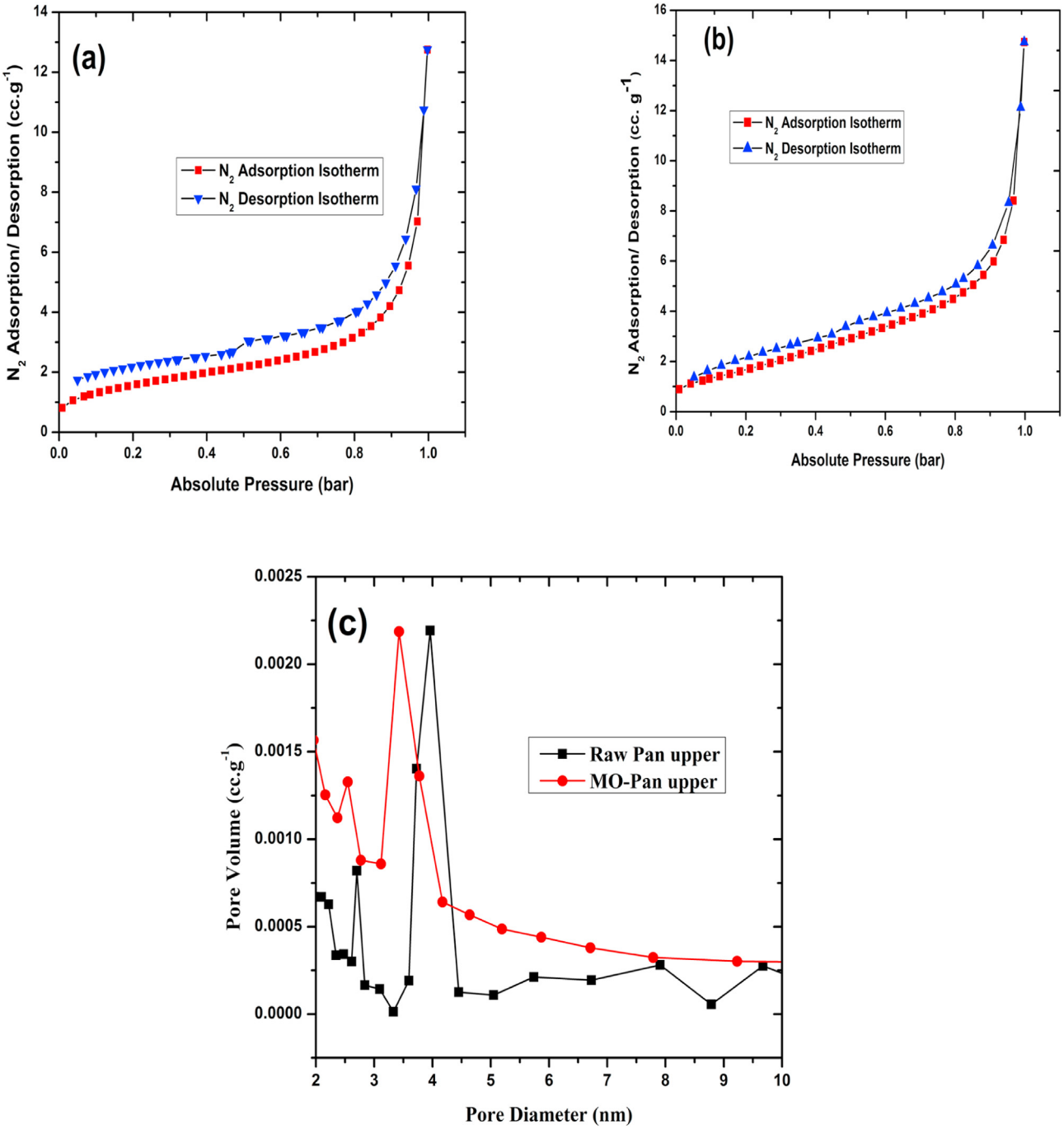

Fig. 4. N_2 adsorption/desorption isotherms measured for raw coal (a), MO-coal (b) and associated raw coal/MO-coal mesopore distribution (c).

hex-acyclic-ring in the structure of coal. It was previously reported the gas adsorption capacity of coal upsurges when the carbon content increases, and at the coal of low carbon content, the rate of gas adsorption slowly increases [64,65], consequently, the slight increase in carbon content in the MO-coal probably further contributed to the enhanced CO_2 adsorption [66]. Fig. 5 shows the CO_2 adsorption in MO-coal reached the maximum capacity when the pressure increased up to 37.7 bar. That is interpreted by that when the pressure increases and the electrostatic interactions enhance, the CO_2 adsorption rate increases. Consequently, the pores expand, and an extraordinary amount of CO_2 is adsorbed [67].

4. Conclusions

CO_2 storage in deep coal seams is the best option to dispose of large amounts of CO_2 that would otherwise emit into the atmosphere (IPCC 2005). Improved affinity of coal to adsorb CO_2 increases CO_2 storage capacity and can enhance methane recovery (via CO_2-ECBM). To increase associated storage capacities of coal, coal samples were prepared and aged with MO. The raw coal and MO-coal were characterized thoroughly to identify surface functional groups, thermal stability, texture, pore size, and specific surface areas, and CO_2 adsorption tests were performed on the coal samples. CO_2 adsorption capacity dramatically increased in MO-

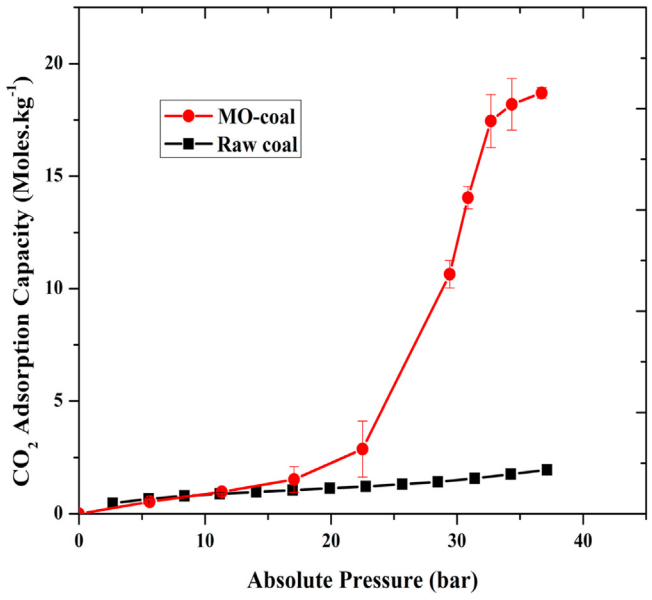

Fig. 5. CO_2 adsorption isotherms of raw and MO-coal at 323 K.

coal (reaching 18.7 mol. kg^{-1} at 37 bar and 323 K, 10 times the adsorption capacity of the raw coal, 1.95 mol. kg^{-1}). Note that these CO_2 adsorption capacities are substantially higher than those reported previously. Note that the molecular structure and the charge distribution on CO_2 molecules significantly affect the CO_2 adsorption on the charged coal. Therefore, this drastic increase in CO_2 adsorption was due to incorporating negative charges on the modified coal surface, which oriented the adsorbed CO_2 molecules parallel to the coal surface. This adsorption orientation strongly increased CO_2–CO_2 intermolecular interactions, leading to the drastic adsorption increase.

This study aids a novel concept of improved CO_2 storage techniques in deep coal seams, and thus the industrial-scale implementation of CO_2 disposal, supporting climate change mitigation efforts.

Declaration of competing interest

The authors declare that they have no known competing financial interests or personal relationships that could have appeared to influence the work reported in this paper.

Acknowledgement

This work was supported by Edith Cowan University (ECU)-Early Career Research Grant G1004709. Also, thanks to Mr. Hamed Akhondzadeh and Dr. Guanliang ZHOU in school of Engineering at ECU for their technical assistance.

Credit author statement

Hussein Rasool Abid: Conceptualization, Methodology, experimental work, Writing, Visualization. Stefan Iglauer: Methodology, Writing – review & editing. Ahmed Al-Yaseri: Review & Editing. Alireza Keshavarz: Conceptualization, Review & Editing, Supervision.

Appendix A. Supplementary data

Supplementary data to this article can be found online at https://doi.org/10.1016/j.energy.2021.120924.

References

[1] Burgess MG, Ritchie J, Shapland J, Pielke Jr R. IPCC baseline scenarios overproject CO2 emissions and economic growth. 2020.
[2] Lashof DA, Ahuja DR. Relative contributions of greenhouse gas emissions to global warming. Nature 1990;344(6266):529–31.
[3] Zhang Y, Lebedev M, Al-Yaseri A, Yu H, Xu X, Iglauer S. Characterization of nanoscale rockmechanical properties and microstructures of a Chinese subbituminous coal. J Nat Gas Sci Eng 2018;52:106–16.
[4] Kiani A, Sakurovs R, Grigore M, Keshavarz A, White S. The use of infrared spectroscopy to determine methane emission rates from coals at atmospheric pressures. Energy Fuels 2019;33(1):238–47.
[5] Abid HR, Rada ZH, Li Y, Mohammed HA, Wang Y, Wang S, et al. Boosting CO2 adsorption and selectivity in metal–organic frameworks of MIL-96(Al) via second metal Ca coordination. RSC Adv 2020;10(14):8130–9.
[6] Abid HR, Rada ZH, Duan X, Sun H, Wang S. Enhanced CO2 adsorption and selectivity of CO2/N2 on amino-MIL-53(Al) synthesized by polar Co-solvents. Energy Fuels 2018;32(4):4502–10.
[7] Shaheen SA, Lipman TE. Reducing greenhouse emissions and fuel consumption: sustainable approaches for surface transportation. IATSS Res 2007;31(1):6–20.
[8] Bachu S. Sequestration of CO2 in geological media: criteria and approach for site selection in response to climate change. Energy Convers Manag 2000;41(9):953–70.
[9] Bachu S. Carbon dioxide storage capacity in uneconomic coal beds in Alberta, Canada: Methodology, potential and site identification. Int J Greenhouse Gas Contr 2007;1(3):374–85.
[10] Leaf-nosed bat. Encyclopædia Britannica. Encyclopædia Britannica Online; 2009.
[11] Ajoma E, Kamali F, Ge J, Hussain F. Effect of CO2-water injection ratio on the Co-optimization of oil recovery and CO2 storage in a swag displacement process. In: 14th greenhouse gas control technologies conference Melbourne; 2018. p. 21–6.
[12] Zhang Q, Ellett KM, Rupp JA, Mastalerz M, Karacan CÖ. Regional- to reservoir-scale evaluation of CO2 storage resource estimates of coal seams. Energy Procedia 2017;114:5346–55.
[13] Shi J, Durucan S. CO2 storage in deep unminable coal seams. Oil Gas Sci Technol 2005;60(3):547–58.
[14] Keshavarz A, Sakurovs R, Grigore M, Sayyafzadeh M. Effect of maceral composition and coal rank on gas diffusion in Australian coals. Int J Coal Geol 2017;173:65–75.
[15] Zhou F, Hussain F, Guo Z, Yanici S, Cinar Y. Adsorption/desorption characteristics for methane, nitrogen and carbon dioxide of coal samples from southeast Qinshui basin, China. Energy Explor Exploit 2013;31(4):645–65.
[16] Sayyafzadeh M, Keshavarz A, Alias ARM, Dong KA, Manser M. Investigation of varying-composition gas injection for coalbed methane recovery enhancement: a simulation-based study. J Nat Gas Sci Eng 2015;27:1205–12.
[17] Sayyafzadeh M, Keshavarz A. Optimisation of gas mixture injection for enhanced coalbed methane recovery using a parallel genetic algorithm. J Nat Gas Sci Eng 2016;33:942–53.
[18] Dake LP. Fundamentals of reservoir engineering. Elsevier; 1983.
[19] Seidle J. Fundamentals of coalbed methane reservoir engineering. PennWell Books; 2011.
[20] Ahmed T. Chapter 1 - fundamentals of reservoir fluid behavior. In: Ahmed T, editor. Reservoir engineering handbook. fifth ed. Gulf Professional Publishing; 2019. p. 1–27.
[21] Mabuza M, Premlall K. Assessing impure CO2 adsorption capacity on selected South African coals: comparative study using low and high concentrated simulated flue gases. Energy Procedia 2014;51:308–15.
[22] Rada ZH, Abid HR, Shang J, Sun H, He Y, Webley P, et al. Functionalized UiO-66 by single and binary (OH)2 and NO2 groups for uptake of CO2 and CH4. Ind Eng Chem Res 2016;55(29):7924–32.
[23] Karanikolos GN, Romanos GE, Vega LF. Editorial: chemical modification of adsorbents for enhanced carbon capture performance. Front Chem 2021;9(90).
[24] Zhao N, Xu T, Wang K, Tian H, Wang F. Experimental study of physical-chemical properties modification of coal after CO2 sequestration in deep unmineable coal seams. Greenhouse Gases: Sci Technol 2018;8(3):510–28.
[25] Romanov VN, Ackman TE, Soong Y, Kleinman RL. CO2 storage in shallow underground and surface coal mines: challenges and opportunities. Environ Sci Technol 2009;43(3):561–4.
[26] Gale J, Freund P. Coal-bed methane enhancement with CO2 sequestration worldwide potential. Environ Geosci 2001;8(3):210–7.
[27] Huang B, Zhao R, Xu H, Deng J, Li W, Wang J, et al. Adsorption of methylene blue on bituminous coal: adsorption mechanism and molecular simulation. ACS Omega 2019;4(9):14032–9.
[28] Almeida CAP, Debacher NA, Downs AJ, Cottet L, Mello CAD. Removal of methylene blue from colored effluents by adsorption on montmorillonite clay. J Colloid Interface Sci 2009;332(1):46–53.
[29] Bhattacharyya KG, Sharma A. Kinetics and thermodynamics of methylene blue adsorption on neem (Azadirachta indica) leaf powder. Dyes Pigments 2005;65(1):51–9.
[30] Tunç Ö, Tanacı H, Aksu Z. Potential use of cotton plant wastes for the removal of Remazol Black B reactive dye. J Hazard Mater 2009;163(1):187–98.

[31] Al Amery N, Abid HR, Wang S, Liu S. Enhancing acidic dye adsorption by updated version of UiO-66. J Appl Mater Technol 2020;1(2):54–62.
[32] Azhar MR, Abid HR, Sun H, Periasamy V, Tadé MO, Wang S. One-pot synthesis of binary metal organic frameworks (HKUST-1 and UiO-66) for enhanced adsorptive removal of water contaminants. J Colloid Interface Sci 2017;490:685–94.
[33] Holkar CR, Jadhav AJ, Pinjari DV, Mahamuni NM, Pandit AB. A critical review on textile wastewater treatments: possible approaches. J Environ Manag 2016;182:351–66.
[34] Ali I, Burakova I, Galunin E, Burakov A, Mkrtchyan E, Melezhik A, et al. High-speed and high-capacity removal of methyl orange and malachite green in water using newly developed mesoporous carbon: kinetic and isotherm studies. ACS Omega 2019;4(21):19293–306.
[35] Liu Z, Zhou A, Wang G, Zhao X. Adsorption behavior of methyl orange onto modified ultrafine coal powder. Chin J Chem Eng 2009;17(6):942–8.
[36] Whitehurst D. A primer on the chemistry and constitution of coal. ACS Publications.
[37] Davidson RM. Molecular structure of Coal11This article was previously published by IEA coal Research, London, as report No. ICTIS/TR 08. In: Gorbaty ML, Larsen JW, Wender I, editors. Coal science. Academic Press; 1982. p. 83–160.
[38] Li D, Li W, Li B. A new hydrogen bond in coal. Energy Fuels 2003;17(3):791–3.
[39] Abotsi GMK, Bota KB, Saha G. Effects OF coal surface charge ON the adsorption and gasification activities OF calcium and potassium. Fuel Sci Technol Int 1993;11(2):327–48.
[40] Kuang Y, Zhang X, Zhou S. Adsorption of methylene blue in water onto activated carbon by surfactant modification. Water 2020;12(2):587.
[41] Zhou Y, Albijanic B, Tadesse B, Wang Y, Yang J, Zhu X. Desulphurization of coals of different ranks in the presence of slimes by reverse flotation. Energy Rep 2019;5:1316–23.
[42] Arif M, Al-Yaseri AZ, Barifcani A, Lebedev M, Iglauer S. Impact of pressure and temperature on CO2–brine–mica contact angles and CO2–brine interfacial tension: implications for carbon geo-sequestration. J Colloid Interface Sci 2016;462:208–15.
[43] Keshavarz A, Badalyan A, Carageorgos T, Bedrikovetsky P, Johnson R. Graded proppant injection into coal seam gas and shale gas reservoirs for well stimulation. In: SPE European formation damage conference and exhibition. All Days; 2015.
[44] Yan G, Bai L, Feng J, Zhang Z. A comparative study on the wettability of two coal samples during deep burial metamorphism. J Chem 2020;2020:5608429.
[45] Wei X, Wang Y, Feng Y, Xie X, Li X, Yang S. Different adsorption-degradation behavior of methylene blue and Congo red in nanoceria/H2O2 system under alkaline conditions. Sci Rep 2019;9(1):4964.
[46] Kalyani DC, Telke AA, Govindwar SP, Jadhav JP. Biodegradation and detoxification of reactive textile dye by isolated Pseudomonas sp. SUK1. Water Environ Res 2009;81(3):298–307.
[47] Yao S, Zhang K, Jiao K, Hu W. Evolution of coal structures: FTIR analyses of experimental simulations and naturally matured coals in the Ordos Basin, China. Energy Explor Exploit 2011;29(1):1–19.
[48] Coates J. Interpretation of infrared spectra, a practical approach. In: Encyclopedia of analytical chemistry: applications, theory and instrumentation; 2006.
[49] Buratti C, Barbanera M, Bartocci P, Fantozzi F. Thermogravimetric analysis of the behavior of sub-bituminous coal and cellulosic ethanol residue during co-combustion. Bioresour Technol 2015;186:154–62.
[50] Saikia BK, Boruah RK, Gogoi PK, Baruah BP. A thermal investigation on coals from Assam (India). Fuel Process Technol 2009;90(2):196–203.
[51] Andersson L, Herring A, Schlüter S, Wildenschild D. Defining a novel pore-body to pore-throat “Morphological Aspect Ratio” that scales with residual non-wetting phase capillary trapping in porous media. Adv Water Resour 2018;122:251–62.
[52] Sing KS, Williams RT. Physisorption hysteresis loops and the characterization of nanoporous materials. Adsorpt Sci Technol 2004;22(10):773–82.
[53] Horikawa T, Do DD, Nicholson D. Capillary condensation of adsorbates in porous materials. Adv Colloid Interface Sci 2011;169(1):40–58.
[54] Zeng Y, Fan C, Do DD, Nicholson D. Evaporation from an ink-bottle pore: mechanisms of adsorption and desorption. Ind Eng Chem Res 2014;53(40):15467–74.
[55] Fan C, Do DD, Nicholson D. On the cavitation and pore blocking in slit-shaped ink-bottle pores. Langmuir 2011;27(7):3511–26.
[56] Yang R, Li D, Li A, Yang H. Adsorption properties and mechanisms of palygorskite for removal of various ionic dyes from water. Appl Clay Sci 2018;151:20–8.
[57] Zou Y, Rodrigues AE. Adsorbent materials for carbon dioxide. Adsorpt Sci Technol 2001;19(3):255–66.
[58] Iglauer S. CO2–Water–Rock wettability: variability, influencing factors, and implications for CO2 geostorage. Acc Chem Res 2017;50(5):1134–42.
[59] Poloni R, Lee K, Berger RF, Smit B, Neaton JB. Understanding trends in CO2 adsorption in metal–organic frameworks with open-metal sites. J Phys Chem Lett 2014;5(5):861–5.
[60] Ralser S, Kaiser A, Probst M, Postler J, Renzler M, Bohme DK, et al. Experimental evidence for the influence of charge on the adsorption capacity of carbon dioxide on charged fullerenes. Phys Chem Chem Phys 2016;18(4):3048–55.
[61] Zhu J, He F, Zhang Y, Zhang R, Zhang B. Fractal analysis in pore size distributions of different bituminous coals. Sci Rep 2019;9(1):18162.
[62] Mastalerz M, Drobniak A, Rupp J. Meso-and micropore characteristics of coal lithotypes: implications for CO2 adsorption. Energy Fuels 2008;22(6):4049–61.
[63] Asgari M, Jawahery S, Bloch ED, Hudson MR, Flacau R, Vlaisavljevich B, et al. An experimental and computational study of CO2 adsorption in the sodalite-type M-BTT (M = Cr, Mn, Fe, Cu) metal–organic frameworks featuring open metal sites. Chem Sci 2018;9(20):4579–88.
[64] De Silva PNK, Ranjith PG. Understanding and application of CO2 adsorption capacity estimation models for coal types. Fuel 2014;121:250–9.
[65] Cheng Y, Jiang H, Zhang X, Cui J, Song C, Li X. Effects of coal rank on physicochemical properties of coal and on methane adsorption. Int J Coal Sci Technol 2017;4(2):129–46.
[66] Ozdemir E, Schroeder K. Effect of moisture on adsorption isotherms and adsorption capacities of CO2 on coals. Energy Fuels 2009;23(5):2821–31.
[67] García EJ, Pérez-Pellitero J, Pirngruber GD, Jallut C. Sketching a portrait of the optimal adsorbent for CO2 separation by pressure swing adsorption. Ind Eng Chem Res 2017;56(16):4818–29.
[68] Ali M, et al. J Colloid Interface Sci 2021. https://doi.org/10.1016/j.jcis.2020.12.058.
[69] Ali M. Fuel Process Technol 2021. https://doi.org/10.1016/j.fuproc.2021.106722.